for different values of $x=\hbar\omega/K_BT$ at four different temperatures 2, 8, 30, and 100°K for situations where the impurity levels overlap the conduction band and where the impurity states are semi-isolated. For the scattering of phonons by the electrons in the conduction state, Ziman's expression for the electron-phonon scattering relaxation time has been used and for the scattering of phonons by the electrons in the bound states, Carruthers' expression has been used.

5. Assuming the additivity of the reciprocal relaxation times and incorporating the electron-phonon scattering relaxation time in the expression for the combined relaxation time, Callaway's theory has been used to calculate the phonon conductivity of the different Sb- and As-doped Ge samples. The correction due to momentum-conserving phonon-phonon and phonon-electron collisions are shown to be negligible. If one takes into account the temperature dependence of the reduced Fermi potential and the density-of-states effective mass, Ziman's scattering can explain the phonon conductivity of the samples for which the electron concentration is higher than 10^{17} cm^{-3} and the impurity levels merge with the conduction band. The decrease in the thermal conductivity with the increase in doping is explained by the change in the deformation potential and the plot of the deformation-potential constant against the electron concentration is shown to be linear. Carruthers scattering, for which phonons are scattered as a result of virtual transitions of the donor electrons between the ground state and threefold-degeneration first excited state, is found to be more appropriate for those samples for which the donor electron concentration is less than 10^{17} cm^{-3}. Values of the shear deformation potential for Carruthers scattering as obtained from the phonon-conductivity data are found to lie between 17.83 and 27.91 eV.

6. For the Sb-doped Ge samples which are compensated by Ga, known as compensated samples, the phonon conductivity has been calculated on the basis of Carruthers scattering which is considered to be more appropriate for the case where compensation may bring the electrons from the conduction band to any state in the energy gap. By adjusting τ_{ep}^{-1} a satisfactory agreement between theory and experiment is obtained. The values of the shear deformation potential for the compensated samples as obtained from thermal conductivity data are 21.2 and 25.27 eV.

ACKNOWLEDGMENTS

The authors are grateful to Dr. A. Kahn, Professor K. S. Singwi, and Professor Vachaspati for their interest in the project.

PHYSICAL REVIEW VOLUME 159, NUMBER 3 15 JULY 1967

Electron Scattering by Pair Production in Silicon

E. O. KANE
Bell Telephone Laboratories, Murray Hill, New Jersey
(Received 2 March 1967)

The energy-dependent rate for inelastic scattering of electrons by production of electron-hole pairs is computed by first-order perturbation theory for silicon using a screened Coulomb interaction with a frequency- and momentum-dependent dielectric function calculated for silicon in the random-phase approximation. The threshold for momentum-conserving pair creation is found to be very close to that determined by energy conservation alone. This follows from the silicon band structure. The absolute scattering rate is close to that obtained experimentally by Bartelink, Moll, and Meyer. Pair production dominates the scattering rate for electrons of energy greater than 6.5 eV above the valence-band maximum. For electrons between 4 and 6.5 eV the scattering rate is dominated by phonon scattering, but energy loss is dominated by pair scattering. Below 4 eV phonon processes dominate inelastic processes as well. The momentum space integrals for pair-creation scattering are performed by a Monte Carlo method. It is found that the calculations with momentum conservation can be reproduced surprisingly well by a simple "random-**k**" approximation, which effectively ignores momentum conservation. This leads to a very simple expression for pair scattering in the form of a two-dimensional energy fold over one-electron state-density functions, a result first obtained by Berglund and Spicer. This simple form facilitates the calculation tremendously and should make calculations for other materials very simple if the state-density function is known. Using this "random-**k**" method, the scattering rate for primary holes is obtained and found to be almost identical with that for primary electrons of comparable energy. The secondary-particle energy distribution functions are also determined for primary holes and electrons. One-electron state-density structure is prominent in these distributions.

I. INTRODUCTION AND CONCLUSIONS

WHEN an electron or hole has an energy relative to its band edge in excess of the band-gap energy, the energetic particle is able to lose energy by creating an electron-hole pair. Because there are three final-state particles, density-of-states considerations lead one to expect that the cross section for pair production will be a strongly rising function of electron energy, at

least within a few electron volts of threshold. These considerations have long been appreciated and the importance of pair production in avalanche breakdown,[1–3] photoemission,[4] and the scattering and energy degradation of high-energy particles is widely recognized. Pair-production effects have also been observed in the quantum yield of photoconductivity.[5] More recently it has been suggested[6] that pair production is an important mechanism in providing oscillator strength at high-photon energies where one-electron direct transitions are expected to be relatively weak.

Pair-production calculations for metals have been made based on the free-electron approximation.[7] This approximation would not be applicable to semiconductors and insulators except at rather high energies because of band-gap effects due to energy conservation.

Some attempts have been made to discuss pair production in semiconductors based on effective-mass models for the conduction and valence bands.[8,9] This type of model is not valid at high enough energies to be useful.

In the present paper we attempt a quantitative calculation of the pair cross section for silicon using pseudopotential energy bands and wave functions. In Sec. II we calculate the scattering rate by first-order time-dependent perturbation theory using a screened Coulomb interaction. The dielectric screening used is both momentum- and frequency-dependent as calculated for the silicon band structure in the random-phase approximation.[10] The multidimensional integrals over $\mathbf{k}$ space are performed by a Monte-Carlo-type calculation as described in the Appendix.

In Sec. IIA the results of the Monte Carlo calculation are compared to the predictions of the free-electron model which is found to be useful for electron energies 8 eV or more above the valence-band maximum.

In Sec. IIB we discuss the threshold for pair production. We find a pair-production threshold of 2.2 eV (relative to the valence band). In other words, the threshold is just one energy gap above the conduction minimum. This result is shown to be consistent with momentum conservation on the basis of the silicon band structure.

In Sec. IIC we compare the absolute value of our pair scattering rate to experiment. At a primary energy of 5.5 eV (relative to the valence band maximum), we find a scattering rate which is within a factor of 2 of the value determined experimentally by Bartelink, Moll, and Meyer.[11] The agreement is probably as good as could be expected for the theoretical calculation.

In Sec. IID we compare the rate of electron scattering by pair creation with the rate of scattering by phonons.

If we assume an optical-phonon scattering length of ~ 60 Å as estimated by Bartelink, Moll, and Meyer,[11] we conclude that above 6.5 eV (relative to the valence maximum) pair-production scattering dominates phonon scattering. Between 4 and 6.5 eV, the phonons dominate as a scattering mechanism but pair creation is the most important energy-loss mechanism. Below 4 eV phonons determine the energy-loss rate also.

In Sec. III we discuss the "random-$\mathbf{k}$" approximation. We have found that within the statistical accuracy the results of our momentum-conserving Monte Carlo calculation can be duplicated by assuming that the dependent momentum $\mathbf{k}_4$ is distributed uniformly over the whole Brillouin zone. In other words, momentum conservation can be ignored. This approximation reduces the 9-dimensional integrals over $\mathbf{k}$ space to a two-dimensional fold in energy space of three one-electron state-density functions. (One for each final-state particle.) Computationally, the 9-dimensional $\mathbf{k}$ integral, which contains a δ function for energy conservation, is tedious to evaluate because the relevant fraction of $\mathbf{k}$ space is so small compared to the total. Consequently, the "random-$\mathbf{k}$" approximation which reduces the integral to two energy dimensions and eliminates the δ function makes the problem computationally trivial.

This approximation has been used previously by Berglund and Spicer.[4]

In Sec. IIIA we compare the results of the Monte Carlo calculations with the "random-$\mathbf{k}$" results.

In Sec. IIIB we use the random-$\mathbf{k}$ approximation to compute the pair-production rate for a primary hole. We find that the scattering rates for electrons and holes are practically identical for energies symmetrical relative to the midgap energy.

In Sec. IIIC we use the random-$\mathbf{k}$ approximation to compute the energy-distribution functions for "secondary" or final-state particles. We find that one-electron state-density structure shows up in these distributions, although it may be distorted or masked by an over-all "envelope" imposed by energy conservation.

The validity of the random-$\mathbf{k}$ approximation has important implications for extending the present calculations to other materials. One needs only the one-

---

[1] P. A. Wolff, Phys. Rev. **95**, 1415 (1954).
[2] W. Shockley, in *Proceedings of the International Conference on Semiconductor Physics, 1960* (Academic Press Inc., New York 1961), p. 81.
[3] G. A. Baraff, Phys. Rev. **135**, A528 (1964).
[4] C. N. Berglund and W. E. Spicer, Phys. Rev. **136**, A1030 (1964).
[5] V. S. Vavilov, J. Phys. Chem. Solids **8**, 223 (1959).
[6] A. Bardasis and D. Hone, Phys. Rev. **153**, 849 (1967).
[7] J. J. Quinn, Phys. Rev. **126**, 1453 (1962).
[8] P. T. Landsberg, in *Lectures in Theoretical Physics* (John Wiley & Sons, Inc., New York, 1966), edited by W. E. Brittin, B. W. Downs, and J. Downs, Vol. VIII-A, p. 313.
[9] D. L. Dexter, *Proceedings of the International Conference on Semiconductor Physics, 1960* (Academic Press Inc., New York, 1961), p. 122.
[10] E. O. Kane (unpublished).
[11] D. J. Bartelink, J. L. Moll, and N. I. Meyer, Phys. Rev. **130**, 972 (1963).

electron state density function. The multiplicative constant might crudely be assumed to be the same as for silicon or more accurately might be determined by a one-parameter fit to experiment.

It appears that the random-$\mathbf{k}$ approach as used here may be applicable to all the "nearly free electron" materials for which a simple pseudopotential works well. On the other hand, it would not be expected that materials with d bands could be treated without important modifications. Coulomb matrix elements between d-like and free-electron-like states would presumably be much smaller than between two free-electron-like states because of the relatively large spread in momentum space of d functions.

II. MONTE CARLO CALCULATION OF SCATTERING DUE TO PAIR PRODUCTION

In this section we describe a calculation of the scattering rate, w, for an electron to produce an electron-hole pair in silicon. The calculation is done using first-order time-dependent perturbation theory with pseudopotential wave functions and energy bands.[12] We use a Coulomb interaction between electrons with dielectric screening. A frequency- and momentum-dependent dielectric constant was used as computed for silicon using the random-phase approximation (RPA).[13]

We calculate $w(E)$ using first-order time-dependent perturbation theory

$$w(E)=\frac{2\pi}{\hbar}\left(\frac{V}{(2\pi)^3}\right)^2\sum_{n_1,n_2,n_3,n_4}\frac{\int d\mathbf{k}_1 d\mathbf{k}_2 d\mathbf{k}_3\,\delta(\mathcal{E}_1(\mathbf{k}_1)-E)}{\sum_{n_1}\int d\mathbf{k}_1\delta(\mathcal{E}_1(\mathbf{k}_1)-E)}\delta(\mathcal{E}_1(\mathbf{k}_1)+\mathcal{E}_4(\mathbf{k}_4)-\mathcal{E}_2(\mathbf{k}_2)-\mathcal{E}_3(\mathbf{k}_3))\times\{|M_a|^2+|M_b|^2-(M_a^*M_b+M_aM_b^*)/2\}, \tag{1}$$

$$M_a\equiv M(1,4;2,3)\quad M_b\equiv M(1,4;3,2), \tag{2}$$

$$M(1,4;2,3)\equiv\int\left\langle\psi_1(\mathbf{r}_1)\psi_4(\mathbf{r}_2)\left|\frac{e^2}{\epsilon|\mathbf{r}_1-\mathbf{r}_2|}\right|\psi_2(\mathbf{r}_1)\psi_3(\mathbf{r}_2)\right\rangle d\mathbf{r}_1 d\mathbf{r}_2, \tag{3}$$

$$\mathbf{k}_1+\mathbf{k}_4=\mathbf{k}_2+\mathbf{k}_3+\mathbf{K}_0, \tag{4}$$

where V is the volume.

State 1 is the initial state, consisting of a primary electron of energy E. In Eq. (1) we average over all initial states with momentum $\mathbf{k}_1$ and band index n_1 having energy E. State 4 is the hole state. We sum over the band index n_4 of the hole but allow the hole momentum to be determined by momentum conservation, Eq. (4). $\mathbf{K}_0$ is a principal lattice vector (which may be zero) to insure that $\mathbf{k}_1$, $\mathbf{k}_2$, $\mathbf{k}_3$, $\mathbf{k}_4$ are all in the first Brillouin zone. States $\mathbf{k}_2$, n_2 and $\mathbf{k}_3$, n_3 are final electron states.

Allowance is made in Eq. (1) for the effect of exchange which gives rise to the matrix-element expression in braces after summing over spins. The indicated sums over n_1, n_2, n_3, n_4 do not include spin.

M is the matrix element of the screened Coulomb interaction. ϵ is the frequency- and momentum-dependent dielectric function.

To indicate more explicitly the way we use the dielectric function, we write the pseudopotential wave functions $\psi_i(\mathbf{r}_i)$ in the form

$$\psi_i(\mathbf{r}_i)=\sum_{\mathbf{K}}a(\mathbf{K},\mathbf{k}_i,n_i)\frac{e^{i(\mathbf{k}_i+\mathbf{K})\cdot\mathbf{r}_i}}{\sqrt{V}}. \tag{5}$$

We also write $1/|\mathbf{r}_1-\mathbf{r}_2|$ in momentum space

$$1/|\mathbf{r}_1-\mathbf{r}_2|=\frac{1}{V}\sum_{\mathbf{q}}\frac{4\pi}{q^2}e^{i\mathbf{q}\cdot(\mathbf{r}_1-\mathbf{r}_2)}. \tag{6}$$

Equation (3) then becomes

$$M(1,4;2,3)=\sum_{\mathbf{K}_1,\mathbf{K}_2,\mathbf{K}_3}a^*(\mathbf{K}_1,\mathbf{k}_1,n_1)a^*(\mathbf{K}_4,\mathbf{k}_4,n_4)\times a(\mathbf{K}_2,\mathbf{k}_2,n_2)a(\mathbf{K}_3,\mathbf{k}_3,n_3)\left(\frac{e^2 4\pi}{q^2V}\right)\frac{1}{\epsilon(q,\omega)}, \tag{7}$$

$$\mathbf{q}\equiv\mathbf{k}_1+\mathbf{K}_1-\mathbf{k}_2-\mathbf{K}_2,\qquad \hbar\omega\equiv\mathcal{E}_1(\mathbf{k}_1)-\mathcal{E}_2(\mathbf{k}_2). \tag{8}$$

Momentum conservation together with Eq. (4) determines $\mathbf{K}_4$ according to

$$\mathbf{K}_1+\mathbf{K}_4+\mathbf{K}_0=\mathbf{K}_2+\mathbf{K}_3. \tag{9}$$

The $\epsilon(q,\omega)$ was obtained from an RPA calculation using pseudopotential energy bands and wave functions for silicon.[10]

The integrals in Eq. (1) were performed by a Monte Carlo method. This part of the calculation is described in more detail in the Appendix. The results are shown as circles in Fig. 1. There is a considerable scatter of the data points due to the statistical fluctuations inherent in a Monte Carlo calculation.

A. Comparison with the Free-Electron Model

In Fig. 1 we show as a dashed line a pair-production calculation using free-electron bands, wave functions,

[12] E. O. Kane, Phys. Rev. **146**, 558 (1966).
[13] S. L. Adler, Phys. Rev. **130**, 1654 (1963); H. Ehrenreich and M. H. Cohen, *ibid.* **115**, 786 (1959).

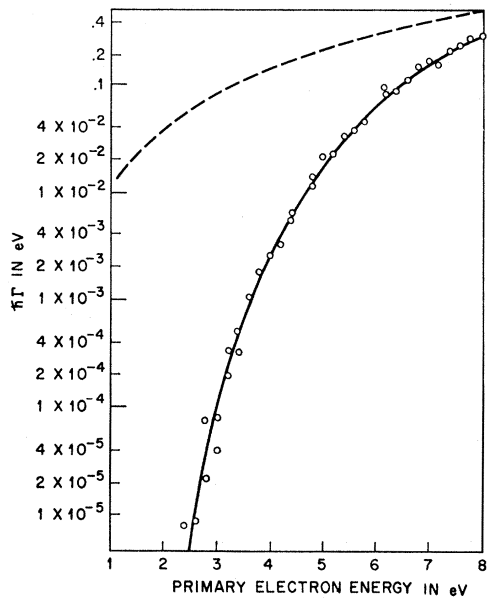

FIG. 1. Scattering rate for pair production by a primary electron in energy units. Γ is the scattering rate or reciprocal lifetime. Electron energy zero is the valence band maximum. Circles are the results of a Monte Carlo calculation. The solid curve is the "random-k" approximation. The dashed curve is pair scattering computed in the free-electron approximation with an electron density corresponding to silicon.

and a dielectric function computed for an electron density appropriate to silicon. The calculation can be carried much further analytically in this case as has been done by Quinn and Ferrell.[7,14] However, Quinn and Ferrell's treatment does not include exchange.

The two curves appear to be coming together at high energy as one would expect, assuming the correction for exchange to be small on this scale. The large reduction of the scattering rate for silicon at low energy is, of course, due to the presence of a band gap.

B. Threshold for Pair Production

In Fig. 1, electron energies are measured relative to the valence band maximum. At low energies the cross section appears to go to zero at a threshold of just twice the band gap, as required by energy conservation. This conclusion differs from predictions based on simple parabolic conduction and valence bands. If the masses are taken equal, the threshold with momentum conservation is 2.5 times the band gap[8] (valence band energy zero). However, it is easily seen that for the band structure of Si, the threshold with momentum conservation is actually very close to twice the band gap.

If we start with a primary electron of 2.2 eV, i.e., twice the band gap, we can locate this electron at $k=(2\pi/a)(0.32,0,0)$.[12] If we take the hole to be at $k=(0,0,0)$ and put two electrons at $k=(2\pi/a)(0.84,0,0)$, we can conserve momentum with the help of a $(2\pi/a)\times(2,0,0)$ reciprocal lattice vector. Feher[15] has located the conduction-band minimum at $(2\pi/a)(0.85,0,0)$, so that the threshold is very nearly equal to twice the band gap. Even if the momentum for which the primary energy equals 2.2 eV were uncertain by as much as $\pm(2\pi/a)(0.2,0,0)$, if one shifts the two final electrons by $\pm(2\pi/a)(0.1,0,0)$ each, the threshold is only increased by 0.1 eV since the longitudinal conduction-band mass is nearly equal to the free-electron mass.

Of course, the scattering rate is very low near threshold so that the effective threshold may be much higher than 2.2 eV and will depend on the experiment being analyzed.

C. Comparison with Experiment

To compare our calculated pair-scattering rates with experiment, we have a pair-production mean free path l_{pr} of 190 Å as determined by Bartelink, Moll, and Meyer.[16] Baraff[3] has analyzed Bartelink, Moll, and Meyer's data more extensively and estimates a value of 270 Å for l_{pr} .For clean silicon the vacuum level is at 5.15 eV as determined by Allen and Gobeli.[17] If we add a thermal spread of the order of 0.5 eV as estimated by Bartelink, Moll, and Meyer,[16] we get an average electron energy of 5.65 eV for their experiment. At this energy we have calculated an average group velocity, v_g, of 0.66 atomic units from the silicon band structure.[18] Using the scattering rate of Fig. 1, we calculate a mean free path, $l_{pr}=v_g/w_{pr}$, of 180 Å. The agreement is probably within the limits of uncertainty of the theoretical calculation.

D. Comparison of Pair Production and Phonon Scattering Rates

If we take an optical-phonon scattering rate of 0.1 eV, (based on a mean free path given by Bartelink, Moll, and Meyer,[16]) we see that the pair scattering rate equals the phonon rate at 6.4-eV electron energy. However, the energy loss in pair production is 2–3 eV per event whereas in phonon scattering it is only 0.05 eV per event.

Taking an energy loss ratio of 50, the energy loss rate to pair production equals the loss to phonons at about 4 eV, primary electron energy. For electrons well below 4 eV in silicon pair production will be quite unimportant in photoemission and in many other experiments as well. A possible exception is avalanche multiplication where extremely small multiplication factors may still lead to breakdown. In this case the

[14] J. J. Quinn and R. A. Ferrell, Phys. Rev. **112**, 812 (1958).

[15] G. Feher, Phys. Rev. **114**, 1219 (1959).

[16] D. J. Bartelink, J. L. Moll, and N. I. Meyer, Phys. Rev. **130**, 972 (1963).

[17] F. G. Allen and G. W. Gobeli, Phys. Rev. **127**, 150 (1962).

[18] E. O. Kane, Proceedings of the International Conference on Semiconductor Physics, 1966, J. Phys. Soc. Japan Suppl. **21** (1966).

effective pair-production energy depends on the maximum in the product of a rapidly falling distribution function and the rapidly rising pair cross section. The effective threshold can only be determined with the use of a very good electron distribution function which is probably rather sensitive to the experimental details.

III. RANDOM-k APPROXIMATION

The Monte Carlo calculations of w are rather tedious. We have tested a much simpler approximation in which we effectively neglect momentum conservation. A similar approach was first taken by Berglund and Spicer.[4]

We still use Eqs. (1) through (4), but we assume that $\mathbf{k}_4$ as given by Eq. (4) is a random variable whose probability $p(\mathbf{k}_4)$ of falling in the energy interval dE_4 in band n_4 is proportional to the density of states $\rho_4(E_4)$ of band n_4.

$$p(\mathbf{k}_4)=\rho_4(E_4)dE_4\Big/\int\rho_4(E_4)dE_4.$$

Of course, $\int\rho_4(E_4)dE_4=2N_c$ where N_c is the number of unit cells and the 2 is for spin. With the above assumption and taking an average value of M^2, we can write Eq. (1) as

$$w_e(E)\equiv\frac{2\pi}{\hbar}\{|M_a|^2+|M_b|^2-(M_a^*M_b+M_aM_b^*)/2\}\frac{\sum_{n_2,n_3,n_4}\int\rho_2(E_2)\rho_3(E_3)\rho_4(E_4)\delta(E+E_4-E_2-E_3)dE_2dE_3dE_4}{8N_c}, \quad (11)$$

where the integral over $\mathbf{k}_1$ in the numerator and denominator of Eq. (1) has cancelled out. The ρ's are assumed to include spin. The sum over n_2, n_3, n_4 converts the ρ_j to total ρ's and the δ function may be integrated over to give

$$w_e(E)=A_e\int\rho(E_2)\rho(E_3)\rho(E_4)dE_2dE_3. \quad (12)$$

$$E=E_2+E_3-E_4;\quad E,E_2,E_3\geq E_F,E_4\leq E_F, \quad (13)$$

$$A_e=\frac{2\pi}{\hbar}\{|M_a|^2+|M_b|^2-(M_a^*M_b+M_aM_b^*)/2\}/(8N_c). \quad (14)$$

E_F represents the Fermi energy which we may take as the top of the valence band. We have used an energy scale with $E_F=0$.

A. Comparison of Random-k and Monte Carlo Calculations

Equation (12) is plotted as the solid line in Fig. (1). Any deviations from the more exact theory are within the random scatter of the Monte Carlo calculation. The fit is accurate not only as to shape but also as to absolute value. An equation similar to (12) was first given by Berglund and Spicer.[4]

The source of this rather surprising agreement probably depends partly on the following considerations. Let $\mathbf{k}_1$, $\mathbf{k}_2$, $\mathbf{k}_3$ be general $\mathbf{k}$ vectors lying in the cubic sector (1/48 of the Brillouin zone). Then if we consider the entire set of cubically equivalent vectors and use Eq. (4) we have

$$\mathbf{k}_4=-Q_1\mathbf{k}_1+Q_2\mathbf{k}_2+Q_3\mathbf{k}_3+\mathbf{K}_0, \quad (15)$$

where Q_i is one of 48 operators which generate cubically equivalent $\mathbf{k}$ vectors. There are evidently 48^3 different values of $\mathbf{k}_4$ in Eq. (15). Of these, 48^2 or 2304 are cubically *inequivalent* (for sufficiently general $\mathbf{k}_1$, $\mathbf{k}_2$, $\mathbf{k}_3$). This large set of values of $\mathbf{k}_4$ will tend to scatter more or less at random throughout the zone. The three integrals over $\mathbf{k}$ space also perform considerable averaging which tends to eliminate any possible structure.

The double fold of the one-electron density of states in Eq. (12) washes out all noticeable structure in the final density of states.

One would expect the "random-$\mathbf{k}$" approach to be least applicable near threshold, however there is no evidence for this in Fig. (1) for energies as close to threshold as computations were feasible. Since the cross section is so very small in this region the exact behavior near threshold seems to be of no practical importance.

The computed values of M^2 were very insensitive to the primary electron energy. The variation from 5 to 8 eV was less than 30%, which is of the order of the statistical uncertainty in the computation.

The success of Eq. (12) in reproducing the more exact Monte Carlo results is very gratifying in that it should make calculations on other materials extremely easy once the one-electron density of states $\rho(E)$ is known.

B. Primary Hole Scattering Rate

We have used the "random-$\mathbf{k}$"[11] approximation to compute the pair-scattering rate for primary holes. We obtain an equation completely analogous to Eq. (12), namely,

$$w_h(E)=A_h\int\rho(E_2)\rho(E_3)\rho(E_4)dE_2dE_3,$$

$$E=E_2+E_3-E_4;\quad E,E_2,E_3\leq E_F,E_4\geq E_F. \quad (16)$$

In all our equations we have used the convention that E refers to the electron energy of a state. The energies of holes are, therefore, $-E$.

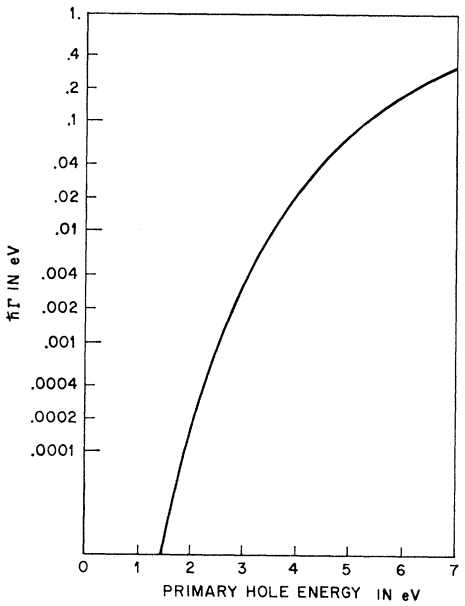

FIG. 2. Scattering rate for pair production by a primary hole in energy units as calculated by the random-**k** approximation. Energy zero is the valence-band maximum.

The scattering rate for holes is shown in Fig. 2. We have arbitrarily used $A_h=A_e$ in this calculation, an untested assumption but one which we feel is probably not too bad in view of the insensitivity of M^2 to primary energy. Even though $A_h=A_e$ one would not necessarily expect $w_h(E)$ to equal $w_e(E)$ for equal energies relative to *midgap* because the density-of-states functions are not symmetrical with energy about the midgap position.[12] Nevertheless, if we line up Figs. 1 and 2 so that the energy 1.1 eV in Fig. 1 coincides with 0 eV in Fig. 2 we see that the curves are virtually identical. This fact suggests that asymmetries observed between electron and hole processes in avalanche breakdown[19] are more likely to be associated with the phonon scattering rate or with the hot-carrier distribution function than with the pair-creation process.

C. Secondary Distribution Functions

We have also used the "random-**k**" approximation to compute the final-state energy distribution function for the secondary particles as a function of the primary particle energy. The secondary distribution functions are given by

$$S_{ee}(E,E_2)=\frac{2\rho(E_2)\int\rho(E_3)\rho(E_4)dE_3}{\int\rho(E_2)\rho(E_3)\rho(E_4)dE_2dE_3},$$

$$S_{eh}(E,E_4)=\frac{\rho(E_4)\int\rho(E_2)\rho(E_3)dE_3}{\int\rho(E_2)\rho(E_3)\rho(E_4)dE_2dE_3}, \tag{17}$$

$$E=E_2+E_3-E_4;\quad E,E_2,E_3\geq E_F,E_4\leq E_F,$$

$$S_{he}(E,E_4)=\frac{\rho(E_4)\int\rho(E_2)\rho(E_3)dE_3}{\int\rho(E_2)\rho(E_3)\rho(E_4)dE_2dE_3},$$

$$S_{hh}(E,E_2)=\frac{2\rho(E_2)\int\rho(E_3)\rho(E_4)dE_3}{\int\rho(E_2)\rho(E_3)\rho(E_4)dE_2dE_3}, \tag{18}$$

$$E=E_2+E_3-E_4;\quad E,E_2,E_3\leq E_F,E_4\geq E_F.$$

$S_{ee}(E,E_2)$ is the distribution function for secondary electrons of energy, E_2, produced by a primary electron of energy E. $S_{eh}(E,E_4)$ is the distribution of secondary holes produced by a primary electron. S_{he}, S_{hh} have analogous meanings for primary holes. S_{ee} and S_{hh} are normalized to two since there are two indistinguishable secondary particles in these cases while S_{eh} and S_{he} are normalized to one.

Plots of S_{ee} and S_{eh} are given in Fig. 3 while S_{he} and S_{hh} are given in Fig. 4.

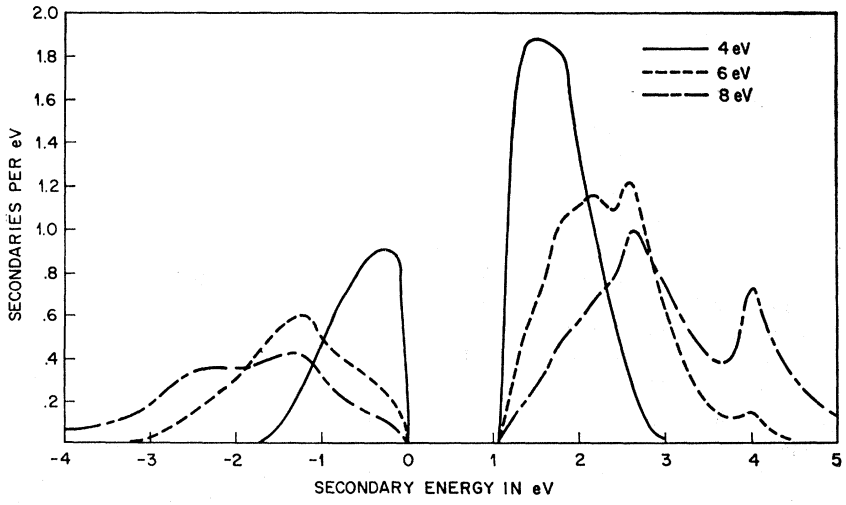

FIG. 3. Energy distribution for secondary particles excited by a primary electron for several primary energies. Secondary electrons normalized to two and holes to one.

[19] C. A. Lee, R. A. Logan, R. L. Batdorf, J. J. Kleimack, and W. Wiegmann, Phys. Rev. 134, A761 (1964).

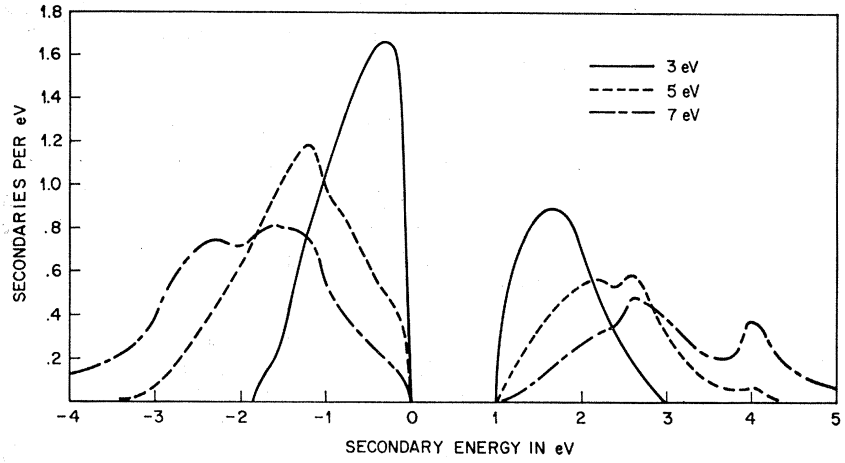

FIG. 4. Energy distribution for secondary particles excited by a primary hole for several primary energies. Secondary holes normalized to two and electrons to one.

The secondary distributions in Figs. 3 and 4 are very similar apart from the normalization which reflects the differing numbers of secondary particles in the two cases. One-electron state-density structure is quite apparent in most of the curves as one would expect from the form of Eqs. (17) and (18). For instance, in formula (17) for $S_{ee}(E,E_2)$ the factor $\rho(E_2)$ is multiplicative which produces most of the structure observed in S_{ee}. The factors under the integral sign are folded which tends to smooth out any structure due to them. The integral provides a strong envelope factor which produces peaks in some curves but the energy location of these peaks are not independent of the primary energy as are the peaks from the $\rho(E_2)$ factor.

ACKNOWLEDGMENTS

The author gratefully acknowledges considerable assistance with the Monte Carlo calculation by Gene Baraff as well as a number of stimulating conversations.

APPENDIX

In this Appendix we describe the Monte Carlo program for performing the integrals in Eq. (1). For a given run the matrix element factors are assumed to be constant so that the principle problem is to evaluate the integrals over delta functions.

The delta functions are represented by rectangles of unit area and width 0.1 eV for the primary energy and 0.4 eV for energy conservation so that energy conservation is satisfied to within ± 0.2 eV.

To illustrate the method we will ignore the sum over band indices in Eq. (1) although all four valence bands and the lowest four conduction bands were actually summed over. This is adequate for primary energies ≤ 8 eV which was the highest energy computed.

The sum over $\mathbf{k}_1$, $\mathbf{k}_2$, $\mathbf{k}_3$ was performed over a coarse mesh of 89 inequivalent cubic boxes in the cubic sector (1/48 of the Brillouin zone). The length of the boxes was $(2\pi/a)$ (0.125). Each box was assigned a weight, $w_f(j)$, equal to the fraction of its volume lying inside the cubic sector. j is the box index running from 1–89. For each box the average energy $\mathcal{E}_n(j)$ and the rms fluctuation of the energy

$$\delta\mathcal{E}_n(j)=\left[\frac{\int_{\text{box}} d\mathbf{k}\,\{\mathcal{E}_n(\mathbf{k})-\mathcal{E}_n(j)\}^2}{\int_{\text{box}} d\mathbf{k}}\right]^{1/2}$$

was computed in advance and stored on tape.

The computation of the integrals over δ functions in Eq. (1) is indicated by the flowchart of Fig. 5 with the operations described in Table I. The boxes in Fig. 5 labeled 0 are arithmetic computations while the boxes T and C involve testing and branching depending on whether the test condition is satisfied or not. C is simply counting so that the total number of selections of mesh boxes j_1, and j_2, j_3 is equal to a prescribed number. Clearly, the essential test is T_{12}, the satisfaction of energy conservation. The intermediate tests greatly speed up the calculation by bypassing later computations when it is already clear that energy conservation would be impossible. Tests T_7 and T_{10} are of this type. In T_7, E_{vm} is the maximum valence-band energy. The energy subscripts such as i in E_i refer to band indices which are summed over in the actual calculation.

Tests T_2 and T_5 limit the computation to primary energies less than a prescribed value, $E_{\max}$. A range of primary energies about 1–2 eV below $E_{\max}$ could be covered in a given run before the statistical fluctuations for the less probable lower energies became too great to tolerate.

In operation O_9, the operators Q_2 and Q_3 convert $\mathbf{k}$ values in the cubic sector into cubically equivalent points (points in the star of $\mathbf{k}$) in the first Brillouin zone. There are 48 different operators, Q_i. The i index is chosen at random. It would be preferable to sum over the entire range of any index with finite range such as the index of the Q_i operators and the mesh indices j. Only the band indices n_i and the j_1 mesh index were actually summed in this way because of the necessity

to limit the total computing time (~6 min per run). The other indices and the $\delta\mathbf{k}$ values were chosen by a random number generating routine which generated numbers between 0 and 1. To get i in Q_i the random number was multiplied by 48 and rounded up.

After $\mathbf{k}_4$ was determined by momentum conservation as indicated in O_9, it had to be mapped back on the cubically equivalent point in the cubic sector of the first Brillouin zone so that the appropriate mesh index $j_4(\mathbf{k}_4)$ could be determined.

After values of $\delta\mathbf{k}$ were determined as in O_4 and O_{11} the energies $\mathcal{E}(\mathbf{k})$ were determined to an accuracy linear in $\delta\mathbf{k}$.

TABLE I. Table of Operations

O_1: Select j_1, mesh index of electron 1.
T_2: Test $\mathcal{E}_1(j_1)-\delta\mathcal{E}_1(j_1)\leq E_{\max}$.
C_3: Counting number of j_1 selections, to be less or equal prescribed number, n_1.
O_4: Calculate $\delta\mathbf{k}_1$, $\mathbf{k}_1=\delta\mathbf{k}_1+\mathbf{k}(j_1)$, random point in mesh box j_1. Calculate $\mathcal{E}_1(\mathbf{k}_1)$.
T_5: Test $\mathcal{E}_1(\mathbf{k}_1)\leq E_{\max}$.
O_6: Add contribution of $\mathbf{k}_1$ point to integral $\int d\mathbf{k}_1\delta(E_1-\mathcal{E}_1(\mathbf{k}_1))$.
O_7: Select j_2, j_3.
T_7: Test $\mathcal{E}_1(\mathbf{k}_1)+E_{vm}\geq\mathcal{E}_2(j_2)+\mathcal{E}_3(j_3)-\delta\mathcal{E}_2(j_2)-\delta\mathcal{E}_3(j_3)$.
C_8: Counting number of j_2, j_3 selections, to be less or equal a prescribed number, n_2.
O_9: Compute $\mathbf{k}_4=Q_2\mathbf{k}(j_2)+Q_3\mathbf{k}(j_3)-\mathbf{k}(j_1)$. Compute $j_4(\mathbf{k}_4)$.
T_{10}: Test $\mathcal{E}_1(\mathbf{k}_1)+\mathcal{E}_4(j_4)+\delta\mathcal{E}_4(j_4)\geq\mathcal{E}_2(j_2)+\mathcal{E}_3(j_3)-\delta\mathcal{E}_2(j_2)-\delta\mathcal{E}_3(j_3)$.
O_{11}: Compute random points $\delta\mathbf{k}_2$, $\delta\mathbf{k}_3$ in mesh boxes j_2, j_3. $\mathbf{k}_2=\delta\mathbf{k}_2+\mathbf{k}(j_2)$; $\mathbf{k}_3=\delta\mathbf{k}_3+\mathbf{k}(j_3)$. Compute $\delta\mathbf{k}_4=Q_2\delta\mathbf{k}_2+Q_3\delta\mathbf{k}_3-\delta\mathbf{k}_1$, Compute $\mathcal{E}_2(\mathbf{k}_2)$, $\mathcal{E}_3(\mathbf{k}_3)$, $\mathcal{E}_4(\mathbf{k}_4)$.
T_{12}: Test $|\mathcal{E}_1(\mathbf{k}_1)+\mathcal{E}_4(\mathbf{k}_4)-\mathcal{E}_2(\mathbf{k}_2)-\mathcal{E}_3(\mathbf{k}_3)|-0.2$ eV ≤ 0.
O_{13}: Add contribution of point $\mathbf{k}_1$, $\mathbf{k}_2$, $\mathbf{k}_3$ to integral $\int d\mathbf{k}_1 d\mathbf{k}_2 d\mathbf{k}_3\delta[(\mathcal{E}_1(\mathbf{k}_1)-E_1)\delta(\mathcal{E}_1(\mathbf{k}_1)+\mathcal{E}_4(\mathbf{k}_4)-\mathcal{E}_2(\mathbf{k}_2)-\mathcal{E}_3(\mathbf{k}_3)]$. Tabulate $\mathbf{k}_1$, $\mathbf{k}_2$, $\mathbf{k}_3$.

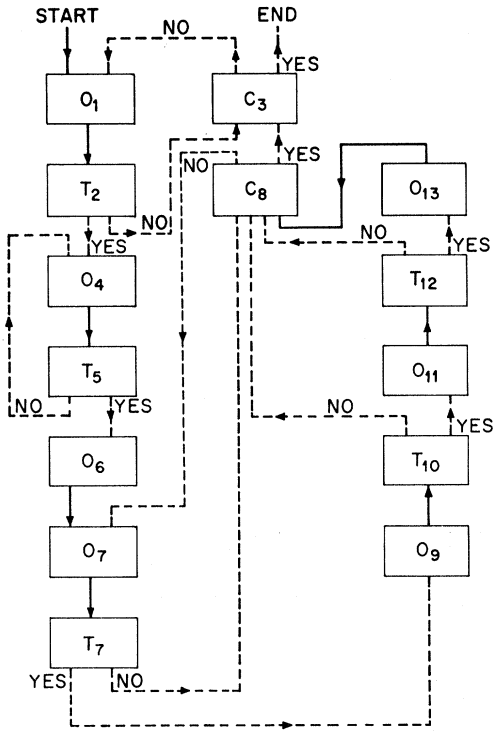

FIG. 5. Flow chart for Monte Carlo program to calculate pair-scattering density of states.

At the conclusion of the run the integral of O_{13} was divided by that of O_6. The set of all $\mathbf{k}_1$, n_1; $\mathbf{k}_2$, n_2; $\mathbf{k}_3$, n_3; $\mathbf{k}_4$, n_4 which satisfied energy conservation was recorded. The Coulomb matrix elements M in Eq. (3) were then computed in a separate program and averaged over the sets of $\mathbf{k}_i$, n_i. In this way a value of $\bar{M}^2$ was found which was strongly weighted in the vicinity of the maximum primary energy $E_{\max}$. Values of M^2 were determined for an $E_{\max}$ of 5 and 8 eV. The variation with primary energy was within the statistical fluctuation (~30%).